

# Excitation Dependence of Steady-State Photoluminescence in CdSe Nanocrystal Films

V. Babentsov,<sup>†</sup> J. Riegler, J. Schneider, M. Fiederle, and T. Nann\*

Freiburger Materialforschungszentrum, Albert-Ludwigs-Universität Freiburg, Stefan-Meier-Strasse 21, D-79104 Freiburg, Germany

Received: April 29, 2005; In Final Form: June 23, 2005

The excitonic and deep-level photoluminescence (PL) in CdSe nanocrystal (NC) films (wurtzite type) was studied under continuous-wave excitation as a function of excitation power, temperature, and time of photoaging. It was shown that the intensity–power dependencies are identical for excitonic and deep-level emissions in a wide temperature range. At low temperatures (80–100 K), both emissions were saturated at the laser power used, which generates more than one exciton per nanocrystal. A transition point from the linear to the saturated region was dependent on the temperature, size, and quality of the NCs. A clear *inverse dependency* between the intensities of excitonic and deep-level emissions was revealed at 80 K over the entire sample area. At room-temperature, the quantum yield dropped significantly and a higher laser power was needed to reach PL saturation. An increase in temperature led to worsening of the reverse dependence between excitonic and deep-level emissions, and at room-temperature, they became uncorrelated. These results can be explained by Auger recombination and also by an increase of *nonradiative recombination* in the surface states with increasing temperature.

## I. Introduction

CdSe nanocrystals (NCs) with dimensions smaller than the diameter of the bulk exciton have attracted increasing interest because of their size dependent optical and electronic properties,<sup>1,2</sup> which are important for applications such as labeling of biomolecules,<sup>3–5</sup> phosphors,<sup>6</sup> light-emitting diodes (LEDs),<sup>7,8</sup> and others. Lasers and high-speed optoelectronic devices use fast excitonic emission, while delayed surface emission has potential applications in biological imaging. Of particular significance are the large quantum yield (QY) of the excitonic (band-to-band) emission and its spectral dependence on the size of the nanocrystal. Recently, premium values of 85% QY have been reported.<sup>9</sup> Nevertheless, such a large QY is a rather unique result. Normally, the *radiative or nonradiative* recombination in the surface states competes with the recombination in the intrinsic excitonic states of NCs at high temperatures.<sup>10–12</sup> Radiative decay times are typically in the nanosecond range for the excitonic emission and reach the millisecond range for surface emissions.<sup>2,10,12–14</sup>

The excitonic emission may drop significantly with temperature due to dissociation of excitons followed by recombination of charges in surface defects.<sup>15,16</sup> Since the pioneering works of Brus's group,<sup>12,17</sup> deep-level photoluminescence (PL) in CdSe NCs has also been ascribed to recombination in surface defects. The donor–acceptor and “trap emission” models have explored this idea over a long period of time. In the donor–acceptor model, a recombination rate depends on the distance between a surface donor and an acceptor and also a spectral position of the PL band maximum is a function of time and excitation power.<sup>12,16,17</sup> The “trap emission” model predicts two deep-level PL bands: the first emission arises when the electron from

selenium dangling bonds recombines with the valence band hole, and the second one is attributed to the  $1S_e$  electron recombination with the hole on a Se dangling bond.<sup>13</sup> Great progress has been achieved due to time-resolved photoluminescence spectroscopy in CdSe NCs.<sup>1,2,10–13</sup>

In this work, we studied the photoluminescence (PL) of an ensemble of CdSe NCs under continuous wave (cw) excitation with respect to three properties, namely, the intensity dependence on the excitation power, temperature, and aging time. Such an approach, coupled with the spatial mapping of the excitonic and deep-level intensities, could give additional insight into the recombination mechanism in CdSe NCs. This was justified by renewed interest in cw PL measurements after the intermittency phenomenon had been found in single NCs.<sup>18</sup>

The cw PL technique easily operates in a wide spectral region from visible to IR with monitoring of excitation power and temperature. It can be used for the spatial mapping of PL intensity at various wavelengths. In addition, it has been demonstrated by Klimov's group that this technique is not sensitive to fast radiative recombination (e.g., biexciton emission);<sup>19</sup> thus, it is well-suited for detection of the radiative recombination in charge excitons and deep-levels.

In this paper, we studied the intensity–excitation dependencies of the excitonic and deep-level emissions in CdSe NCs at various temperatures. Both of these emissions demonstrated the same intensity–power dependence. At 80 K, a region of PL saturation could be reached at the laser power applied. With an increase in temperature and/or increased surface worsening, higher excitations were needed for transition to a saturation region. The intensity–power dependence at low excitation was linear at 80 K, but it was slightly *sublinear* at room-temperature (RT). In the previous studies, this fact was not underlined, and this dependency was always considered to be linear. The sublinear dependency was observed at high temperatures, when trapping to long-living states outside of the NCs is more probable. We explain the observed saturation by attributing it

\* Corresponding author. Fax: +49-761-203-4768. E-mail address: thomas.nann@fmf.uni-freiburg.de.

<sup>†</sup> Permanent address: Institute for Semiconductor Physics, Pr. Nauki 45, Kiev 03028, Ukraine.

to Auger recombination when more than one exciton per nanocrystal could be excited at low temperatures. A clear *inverse dependence* between the intensities of excitonic and deep-level emissions was revealed at 80 K over the entire sample area. At room-temperature, higher laser power was needed to reach the saturation region. An increase of temperature led to worsening of the reverse dependence between the excitonic and deep-level emissions, and at room-temperature, they become uncorrelated. These results are explained by an increased role of *nonradiative recombination* in the surface states at higher temperatures. First, we focused on the intensity dependence of the number of excitations in NCs; then, we emphasized that at room-temperature this dependence was *slightly sublinear* and the total emission was weak as compared with the low-temperature emission. Finally, the three-level rate equation model with a nonradiative recombination term was used for the fitting of experimental results.

The paper is organized as follows: section I is the Introduction, and in section II the CdSe NC samples and experimental details are described. In section III, the experimental results are presented followed by discussion and computer modeling. Finally, section IV presents a short conclusion.

## II. Experimental Section

The spherical wurtzite type CdSe NCs were synthesized according to a wet chemical procedure that was previously described.<sup>20</sup> The samples for luminescence characterization were prepared by placing small droplets of diluted chloroformic dispersions of CdSe NCs onto clean glass plates in air. The samples were immediately placed in the dark in a pumped and cooled chamber of the cryostat. Thus, we avoided uncontrolled photooxidation and photodarkening. In general, the PL efficiency of the dried CdSe NCs films was lower than that in a freshly deposited drop, similar to the result observed earlier.<sup>21,22</sup> The PL efficiency of CdSe NCs in films probably depends on the disordering of a ligand layer.<sup>22</sup> In our study, the NC surface was stable because of low residual pressure in the chamber ( $10^{-5}$  Torr), and we repeatedly obtained the same PL spectra when samples were reversibly cooled and heated. The temperature in the cryostat was regulated by the flow of nitrogen with the precision of  $\pm 1$  °C.

The PL was excited at 488 nm with an Ar laser in the power range 0.1–100 mW. The laser beam was focused onto a spot of approximately 20  $\mu\text{m}$  in diameter with a photoobjective which was also used for collection of the PL emission. In monolayered films with the lowest density of NCs, approximately 100–200 of the NCs are simultaneously excited.<sup>17</sup> Since we studied the excitation dependence of cw PL at low temperatures, special attention was paid to ensure that the observed results are not due to the sample heating or photodarkening. The laser beam was focused onto the front side of a transparent substrate covered by a thin film of NCs which absorbed  $\approx 1/1000$  of the laser power due to a small total cross section of NCs compared to the beam cross section; the rest of the power was released far from the cooled NC sample. The experiments were performed at decreasing and increasing excitation power, giving the same results. In contrast, the PL power dependencies for 1.9 and 3.2 nm radius NCs were different at the same excitation. All these facts demonstrate that the obtained results do not originate from the heating of NCs due to the light absorption.

## III. Results and Discussion

### 1. Dependence of PL on Excitation Power, Temperature, and Time of Photoaging.

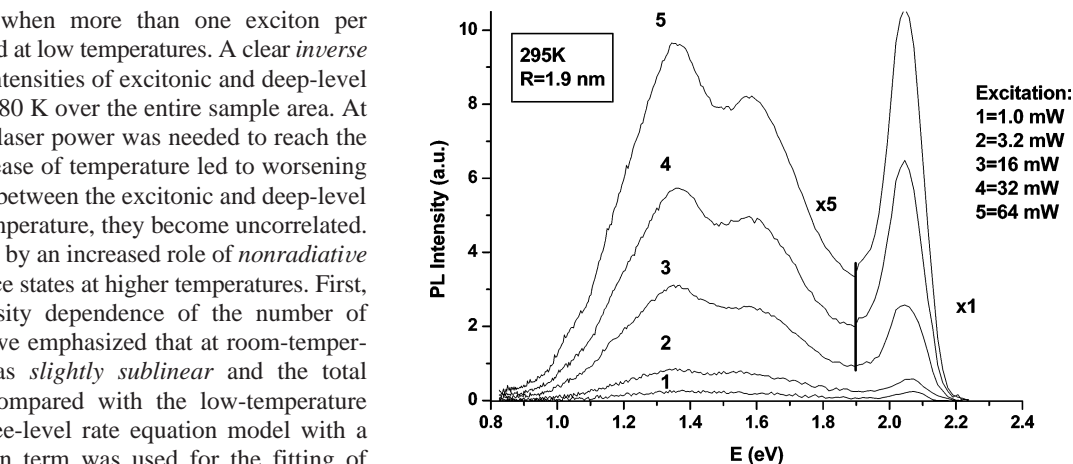


**Figure 1.** Intensity dependence of the PL for wurtzite CdSe NCs with  $R = 1.9$  nm at 295 K. (Note that deep-level emission intensity is multiplied by a factor of 5.)

of the PL spectra from the film composed of 1.9 nm radius ( $R$ ) wurtzite CdSe NCs at 295 K measured at the increased excitation power. The analogous spectra, recorded at two different excitation powers, have been reported earlier for *zinc blend* CdSe NCs ( $R = 2$  nm) prepared by chemical solution deposition (CD).<sup>16</sup> In general, the spectra of wurtzite CdSe NCs differs from those presented earlier for the *zinc blend* CD CdSe NCs in the following two ways: (1) because of better surface passivation, the intensity of the band-to-band (excitonic) line is much stronger than that in CD NCs; (2) not one wide and structureless PL band but two PL bands are resolved in the near-IR spectral region. Details about this phenomenon will be presented elsewhere.

The spectra presented in Figure 1 also demonstrate another important feature, namely, that the PL intensity at every wavelength increases at the same rate; that is, the intensity–power dependencies *are identical* for the excitonic and deep-level emissions. Such behavior of these two emissions was observed in a wide temperature range from 80 to 295 K (not shown). This fact is especially important for an analysis of the deep-level PL emission. In the earliest studies of the PL from NCs imbedded in a glass matrix and from chemically deposited NCs, the position of the deep-level emission in the spectrum was dependent on the excitation power.<sup>12,16,17</sup> The intensity–power dependence of the integrated spectral area at various temperatures is shown in Figure 2 for films containing 1.9 and 3.2 nm radius CdSe NCs at 80 and 295 K, respectively. One can see that PL intensity saturated for *bigger* NCs at *lower* power. Actually, the results were often dependent on uncontrolled conditions such as the influence of air and the amount of time that passes before samples have been placed into a vacuum chamber of the cryostat. The results shown in Figure 2 reflect a typical case when samples have been mounted in the pumped cryostat immediately after drop casting. Figure 2 also demonstrates that the total emission intensity at RT is much less than that at 80 K and, at this temperature, the intensity–power curves do not saturate at the power used in these experiments. Note that the intensity–power curve for 3.2 nm radius NCs at RT (open circles) is *sublinear* and it obeys the power law ( $I_{\text{PL}} \approx I_{\text{EX}}^\alpha$ ) with  $\alpha = 0.8$ , where  $I_{\text{PL}}$  is the total spectral area and  $I_{\text{EX}}$  is the excitation power. The solid lines in Figure 2, which represent simulations of the experimental results, are *linear* in the presaturated region. The procedure of fitting the PL intensity dependence on excitation power at 80 and 295 K will be discussed later in section III-3.

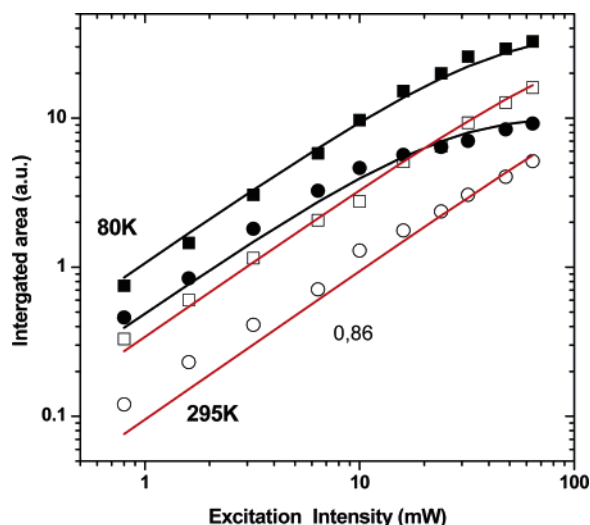


**Figure 2.** Dependencies of the total integrated emission on excitation at 80 K (solid squares and solid circles) and at 295 K (open squares and open circles) for the films containing 1.9 and 3.2 nm radius NCs, respectively.

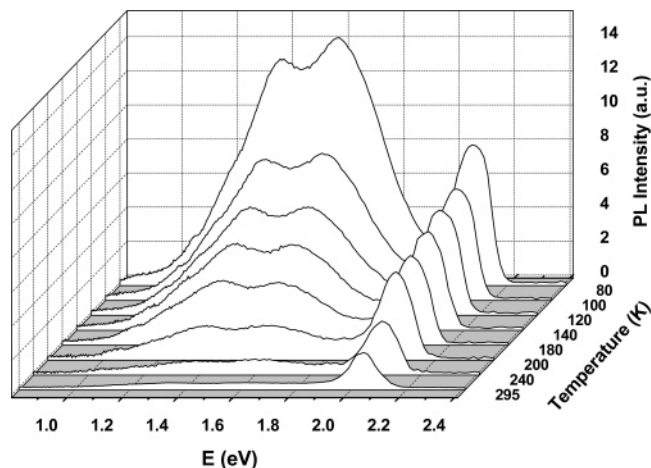


**Figure 3.** Temperature dependence of the PL for CdSe NCs ( $R = 1.9$  nm) at the excitation power 15 mW.

The temperature dependence of the PL demonstrates that the QY dropped mainly due to quenching of the deep-level PL bands; at RT, only the excitonic PL band remained in the spectrum (see Figure 3). This means that nonradiative recombination preferentially competed with the radiative recombination in the deep-levels. A detailed simulation of this PL quenching with temperature will be presented in a separate paper.

A similar quenching, that is, a faster dropping deep-level PL, is expected during the initiation of the intensity–power measurement if an increase in excitation leads to an increase in temperature. This would also decrease the ratio of deep-level to excitonic emission at high powers, which in fact remained unchanged in all measurements, confirming that heating was practically less than 5 K (see Figure 1).

Quasi-saturation of emission could also be observed with worsening of the NC surface or passivation layer during the course of measurements. In this case, PL would be reduced, as compared with that of a perfect NC, due to thermo- or photodarkening effects.<sup>21,22</sup> To check if photodarkening really occurred in our measurements, the samples were photoaged at

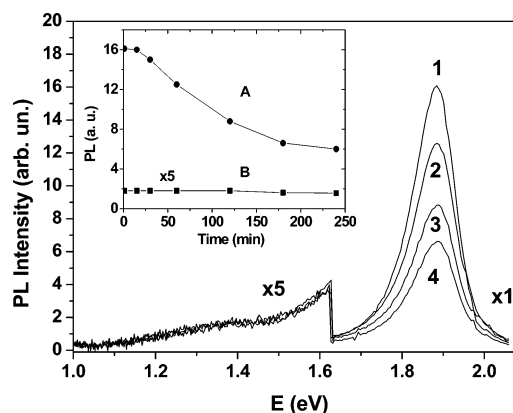


**Figure 4.** Dependence of the PL spectra of the 3.2 nm radius NCs on the aging time (curve 1, 1 h; curve 2, 2 h; curve 3, 4 h; and curve 4, 5 h) at room-temperature. The inset shows the variation of the intensity with time. Line A represents excitonic emission, and line B represents deep-level emission. (Note that deep-level emission intensity is multiplied by a factor of 5.)

a power of 100 mW for 1–6 h at various pressures ( $p$ ) and temperatures ( $T$ ). At  $p = 10^{-5}$  Torr and  $T = 80$  K, the PL spectrum remained unchanged for 6 h, but at  $p = 10^{-3}$  Torr and  $T = 295$  K, for the same time, the excitonic emission dropped significantly. More time was needed to reduce the deep-level emission. Figure 4 shows a typical room-temperature photoaging of a 3.2 nm radius NC film after 1, 2, 3, and 6 h, when only the excitonic band decreased, while the deep-level emission remained practically unchanged. The inset in this figure shows the aging curves of excitonic (A) and deep-level (B) emissions. These results agree with the previously observed photodarkening effect.<sup>13,21</sup> In other words, photoaging led to results which are opposite to those found for an increase in temperature. The absence of a blue shift in the spectra of photoaged NCs in Figure 4 suggests that the photoinduced defects did not cause a reduction in the volume of the NCs due to oxidation, while the degradation of excitonic emission points to destruction of a surface passivation layer.

**2. Mapping of PL Intensity.** The intensities of the excitonic ( $I_{\text{ex}}$ ) and deep-level emissions ( $I_{\text{deep}}$ ) were measured in a spatially resolved mode for the entire NC film. The intensity of the deep-level emission,  $I_{\text{deep}}$ , was quite weak in some areas, while the intensity of the excitonic emission,  $I_{\text{ex}}$ , in these areas was strong. Such a reverse dependence was only observed at 80 K and not at room-temperature. In Figure 5,  $I_{\text{deep}}$  is plotted as function of  $I_{\text{ex}}$  for the film composed of 1.9 nm radius NCs at 80 and 295 K with 1054 points. From this figure, an inverse correlation between  $I_{\text{deep}}$  and  $I_{\text{ex}}$  at 80 K is obvious; the correlation follows the relationship  $I_{\text{ex}}(80 \text{ K}) = C - I_{\text{deep}}(80 \text{ K})$ , where  $C$  is a constant which represents an integrated spectral area. At room-temperature, this dependence is not valid; the values of  $C$  are small and not constant over the NC film.

These results can only be explained if the nonradiative recombination is quite rare in every ensemble of NCs at 80 K, but they are consistent with radiative recombination at room-temperature. This inhomogeneous nonradiative recombination can be explained by defective states in every NC.

**3. Fitting of the PL Intensity–Excitation Power Dependence.** An explanation of the origin of the observed PL saturation at 80 K and its absence at room-temperature can be made by the estimation of the number of excitations in one NC under the experimental conditions. The population of NCs is a



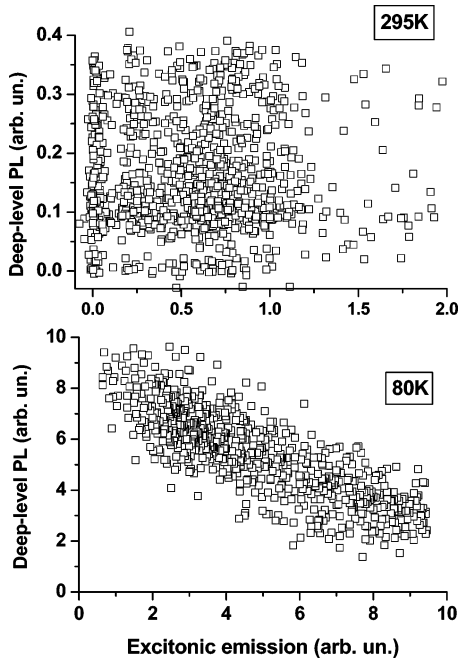


**Figure 5.** Inverse correlation at 80 K (lower panel) and the absence of correlation at 295 K (upper panel) between the excitonic and deep-level emissions.

random process.<sup>24</sup> The mean number of excitons per NC at cw excitation can be written as

$$\bar{N} = \frac{\tau_{\text{ex}} \sigma}{A h \nu} P = \alpha P \quad (1)$$

where  $\tau_{\text{ex}}$  is the lifetime of an exciton,  $\sigma$  is the absorption cross section of the NCs,  $h\nu = 2.54$  eV is the quantum energy at 488 nm,  $A$  is the cross-sectional area of the beam, and  $P$  is the laser power.

In general, the total decay rate of excitation ( $1/\tau_{\text{ex}}$ ) can be represented as the following sum of the radiative ( $1/\tau_{\text{rad}}$ ) and nonradiative ( $1/\tau_{\text{nonrad}}$ ) rates of decay:  $1/\tau_{\text{ex}} = 1/\tau_{\text{rad}} + 1/\tau_{\text{nonrad}}$ . We supposed, based on the experimental results such as high PL intensity and reverse dependence between the excitonic and deep-level emissions, that at low temperature  $\tau_{\text{ex}}$  reaches its maximum value of  $\tau_{\text{ex}} \approx \tau_{\text{rad}} \approx 50$  ns (see Crooker et al.<sup>10</sup>). The absorption cross sections at 488 nm could be taken from ref 25 as  $\sigma(1.9 \text{ nm}) = 10^{-15} \text{ cm}^2$  and  $\sigma(3.2 \text{ nm}) = 8 \times 10^{-15} \text{ cm}^2$ , respectively. The laser spot size was  $\approx 20 \mu\text{m}$ , and the laser power varied over the interval 5–100 mW. Under these conditions, the maximal number of electron–hole pairs per NC could reach 2 for  $R = 1.9$  nm and 14 for  $R = 3.2$  nm. The later value corresponds to strong saturation of the single exciton PL intensity caused by the Auger recombination process.<sup>12,18</sup>

At RT, a single exciton lifetime,  $\tau_{\text{ex}}$ , for NCs could be smaller than 20 ns, especially for 3.2 nm radius NCs, due to excitonic dissociation and activation of nonradiative recombination. The experimental conditions did not fulfill the requirement to generate two excitations per NC, and saturation of the PL was not observed (see curves corresponding to 295 K in Figure 2).

The second significant feature of the excitation dependence at RT is its sublinear dependency on power,  $I_{\text{PL}} \approx I_{\text{EX}}^\alpha$  with  $\alpha = 0.8$ – $0.9$  (see Figure 2). This was observed in the PL measurements as well as in the absorption–pump dependencies demonstrated by Klimov et al.<sup>26</sup> and El-Sayed et al.<sup>27</sup> The explanation of this sublinearity suggests a decrease in light absorption in charged NCs due to an electric field effect.<sup>20,21,26,27</sup>

Trapping by a surface defect of a NC can only be achieved if an electron has enough energy to overcome the potential barrier or to tunnel through it. At low temperatures, such states are rare. This should lead to a linear intensity–power dependence of emissions from an ensemble of NCs at low temperatures.<sup>28</sup>

In contrast to this, at RT, an electron can more easily overcome the potential barrier to being trapped at a surface defect of a NC. In addition, many NCs in an ensemble can be charged, thus leading to a reduced cross section of light absorption. Consequently, the PL intensity dependence on laser power at RT should be *sublinear*.

If  $n$  NCs are excited with the power  $P$ , various numbers of excitations are present in every NC from a given ensemble of NCs.<sup>18,24,29</sup> For the Poisson distribution, the number of neutral NCs which contain  $N$  excitons per unit of time is  $n(N) = n \bar{N}^N e^{-\bar{N}} / N!$ . At low excitation, e.g., for  $\alpha P = 0.1$ , approximately 90.5% of NCs in the ensemble contain 0 excitons,  $n(0) = n e^{-\alpha P}$ . The majority of the remaining NCs, approximately 8.5%, contain 1 exciton, and  $\approx 1\%$  of NCs contain 2 excitons,  $n(2) = n (\alpha P)^2 e^{-\alpha P}$ .

Thus, at low excitation, the generation rate of single excitons is *linear* with respect to the power,  $n(1) \approx n \alpha P$ . With an increase in the excitation power, the percentage of NCs that contain two excitons increases to 36.6% at  $\alpha P = 1$ . This leads to saturation of a single exciton emission, which is proportional to  $n(1) = n(1 - e^{-\alpha P})$ . The rate of dissociation of single excitons and the rate of capture of charges by deep-level defects is also proportional to  $n(1) = n(1 - e^{-\alpha P})$ ; that is why a deep-level emission saturates at the same power as a single exciton emission. The lifetime of bi-excitons is much shorter than the single exciton's lifetime due to Auger recombination, and their emission was not detected in the integrated cw PL spectra.<sup>12</sup> Thus, the integrated spectral area,  $I_{\text{total}}$ , at any laser power is a sum of the single exciton and deep-level emissions for a given temperature and it can be represented by the equation<sup>12,23</sup>

$$I_{\text{total}} = C(T)(1 - e^{-\alpha(T)P}) \quad (2)$$

where  $C(T)$  and  $\alpha(T)$  are the fitting parameters for comparison with experimental data. We used eq 2 to fit the intensity–power curves, which are presented in Figure 2 (solid lines). For the low-temperature results, a linear dependence followed by a region of saturation was simulated with  $\alpha_1(80 \text{ K}) = 0.03$  and  $\alpha_2(80 \text{ K}) = 0.05$ , respectively, for the NCs with  $R = 1.9$  and 3.2 nm. Knowing  $\alpha_1(80 \text{ K})$ ,  $\alpha_2(80 \text{ K})$ , and the cross sections  $\sigma(1.9 \text{ nm}) = 10^{-15} \text{ cm}^2$  and  $\sigma(3.2 \text{ nm}) = 8 \times 10^{-15} \text{ cm}^2$ , we computed the lifetimes,  $\tau_{\text{ex}}(1.9 \text{ nm}) = 38.4$  ns and  $\tau_{\text{ex}}(3.2 \text{ nm}) = 8$  ns, using eq 1. The obtained value of  $\tau_{\text{ex}}(80 \text{ K}) = 38.4$  ns agrees well with the radiative lifetime of excitation at 80 K reported earlier for similar CdSe NCs by Klimov et al.<sup>10</sup> This provided us with an additional argument that at low temperatures we can neglect nonradiative recombination in CdSe NCs.

The RT experimental curves were fit with  $\alpha_1(295 \text{ K}) = 0.009$  and  $\alpha_2(295 \text{ K}) = 0.003$ , respectively, for the 1.9 and 3.2 nm radius NCs (see Figure 2). Using  $\alpha_1(295 \text{ K})$  for the computation of the RT lifetime in the 1.9 nm radius NCs, we obtained  $\tau_{\text{ex}}(295 \text{ K}) = 11.5$  ns. Comparison of the lifetimes at 80 K and 295 K has shown that at RT the average number of single excitons per one NC is less than one due to an additional nonradiative recombination in the CdSe NCs and also that we cannot neglect this recombination and trapping in the analysis of the recombination at high temperatures.

Such an analysis has already been done for CdSe NCs in the framework of a simple rate equation model by Kuno et al.,<sup>30</sup>

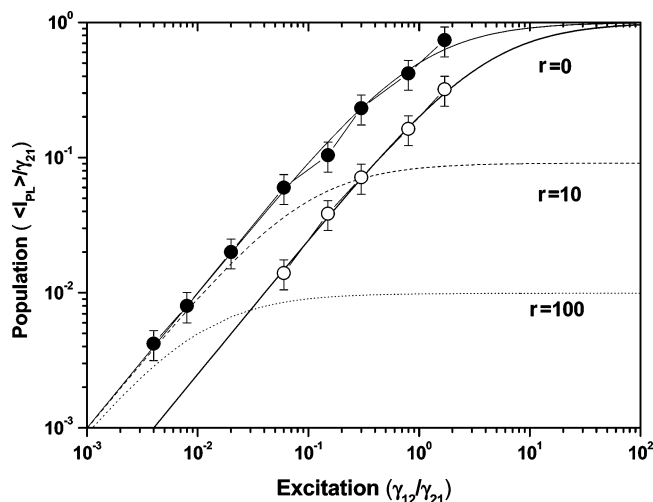


**Figure 6.** Modeling of the integrated spectral intensity dependence on excitation for the 3.2 nm radius NCs using the rate equation model with various escape rates,  $r$ , to the outer states (solid, dashed, and dotted lines) and various nonradiative rates (solid line, see text). The solid circles represent the experiment at 80 K, and the open circles represent the experiment at 295 K.

who paid attention to long-time charge trapping by defects outside of NCs. In this work, we stressed the role of *nonradiative recombination* in the CdSe NCs at high temperatures. A standard system for the population of three levels at steady state in this case of solely excitonic emission is

$$\frac{dn_1}{dt} = -\gamma_{12}n_1 + \gamma_{21}n_2 = 0 \quad (3)$$

$$\frac{dn_2}{dt} = \gamma_{12}n_1 - (\gamma_{21} + \langle\gamma_{on}\rangle)n_2 + \langle\gamma_{off}\rangle n_3 = 0 \quad (4)$$

$$\frac{dn_3}{dt} = \langle\gamma_{on}\rangle n_2 - \langle\gamma_{off}\rangle n_3 = 0 \quad (5)$$

where  $n_1$  and  $n_2$  are, respectively, the highest level for holes and the lowest level for electrons,  $n_3$  is the level outside of a NC for electron capture for the “off” period of intermittency,  $\gamma_{12} = \gamma_{21} = 1/\tau_{ex}$  are the excitonic generation and recombination rates, respectively, and  $\gamma_{on}$  and  $\gamma_{off}$  are the rates of carrier escape and return to/from the  $n_3$  level, respectively. A nonradiative rate of recombination ( $\gamma_{nonrad}$ ) can be introduced via the expression  $\gamma_{21} = \gamma_{rad} + \gamma_{nonrad} = 1/\tau_{rad} + 1/\tau_{nonrad}$ , where  $\gamma_{rad}$  is the rate of radiative recombination. A relative fraction of the radiative recombination,  $I_{PL}/\gamma_{21}$ , was obtained as a solution of eqs 3–5 and is simply the population of level  $n_2$  at steady state.

$$\frac{\langle I_{PL} \rangle}{\gamma_{21}} = n_2 = \left( 1 + \frac{\gamma_{21}}{\gamma_{12}} + \frac{\langle\gamma_{on}\rangle}{\langle\gamma_{off}\rangle} \right)^{-1} \quad (6)$$

In Figure 6 the population  $n_2$  is plotted against the recombination-to-generation ratio,  $\gamma_{21}/\gamma_{12}$ , for various values of  $r = \gamma_{on}/\gamma_{off}$  and  $\gamma_{nonrad}$ . One can see that the low-temperature intensity–power dependence was fit with the assumptions that the average “on” and “off” times in an ensemble of NCs are equal,  $r = 1$ , and the nonradiative rate is small,  $\gamma_{21} \approx \gamma_{rad}$ . The RT curve was well fit with  $\gamma_{nonrad} = 20\gamma_{rad}$ , which corresponds to the observed 24-fold decrease of PL intensity with temperature. Note that  $r = 1$  was chosen tentatively, especially at RT; a real relationship between the intermittency effect in a single NC and the intensity of emission from an ensemble of NCs

still needs to be established.<sup>26,27,31,32</sup> To get a sublinear intensity–power dependence, we assumed  $\gamma_{12}(295 \text{ K}) = \gamma_{12}(80 \text{ K})^{0.8-0.9}$  due to an increased number of charged excitons in an ensemble of NCs. At low temperatures, nonradiative losses are small, and the term  $\gamma_{21}n_2$  represents a pure radiative rate of recombination which linearly increases at low laser powers. These cases were unambiguously observed in this work in drop cast films containing CdSe NCs with  $R = 1.9 \text{ nm}$ .

#### IV. Conclusion

In this paper, an important case of recombination in CdSe NCs under continuous wave excitation was experimentally and theoretically investigated. It was shown for the first time that the intensity–power dependence *could be identical* for the excitonic and deep-level emissions in a wide temperature range (80–295 K). Saturation of the intensity–power dependence was explained by Auger recombination of excitons at low rates of nonradiative loss. A sublinear intensity–power dependence observed at RT suggests that charge excitons could be created when electrons overcome a potential barrier to the states outside of NCs. Spatial mapping of the PL intensities revealed a reverse correlation between the excitonic and deep-level emissions at low temperatures and their uncorrelated behavior at RT due to an increased role of nonradiative recombination. Surface defects responsible for the thermally activated nonradiative losses could appear due to an occasional disordering of the ligand layer in CdSe NCs during film preparation.

#### References and Notes

- Alivisatos, A. *Science* **1996**, 271, 933.
- Efros, A. L.; Rosen, M.; Kuno, M.; Nirmal, M.; Norris, D. J.; Bawendi, M. G. *Phys. Rev. B* **1996**, 54, 4843.
- Bruchez, M., Jr.; Moronne, M.; Gin, P.; Weiss, S.; Alivisatos, A. P. *Science* **1998**, 281, 2113.
- Chan, W. C. W.; Nie, S. *Science* **1998**, 281, 2016.
- Riegler, J.; Nick, P.; Kielmann, U.; Nann, T. *J. Nanosci. Nanotechnol.* **2003**, 3, 380.
- Lee, J.; Sundar, V. C.; Heine, J. R.; Bawendi, M. G.; Jensen, K. F. *Adv. Mater.* **2000**, 12, 1102.
- Colvin, V. L.; Schlamp, M. C.; Alivisatos, A. P. *Nature* **1994**, 370, 354.
- Dabbousi, B. O.; Bawendi, M. G.; Onitsuka, O.; Rubner, M. F. *Appl. Phys. Lett.* **1995**, 66, 1316.
- Qu, L.; Peng, X. *J. Am. Chem. Soc.* **2002**, 124, 2049–54.
- Crooker, S. A.; Barrick, T.; Hollingsworth, J. A.; Klimov, V. I. *Appl. Phys. Lett.* **2003**, 82, 2793–5.
- Wang, X.; Qu, L.; Zhang, J.; Peng, X.; Xiao, M. *Nano Lett.* **2003**, 3, 1103–6.
- Chestnoy, T.; Harris, T. D.; Hull, R.; Brus, L. E. *J. Phys. Chem.* **1986**, 90, 3393–9.
- Underwood, D. F.; Kippeny, T.; Rosental, S. J. *J. Phys. Chem. B* **2001**, 105, 436–43.
- Dahan, M.; Laurence, T.; Pinaud, F.; Chemla, D. S.; Alivisatos, A. P.; Sauer, M.; Weiss, S. *Opt. Lett.* **2001**, 26, 825–7.
- Gindele, F.; Westphäling, R.; Woggon, U.; Spanhel, L.; Pratschek, V. *Appl. Phys. Lett.* **1997**, 71, 2181–3.
- Lifshitz, E.; Dag, I.; Litvin, I.; Hodes, G.; Gorer, S.; Reisfeld, R.; Zelman, M.; Minti, H. *Chem. Phys. Lett.* **1998**, 288, 188–196.
- Kortan, A. R.; Hull, R.; Opila, R. L.; Bawendi, M. G.; Steigerwald, M. L.; Carroll, P. J.; Brus, L. E. *J. Am. Chem. Soc.* **1990**, 112, 1327–32.
- Nirmal, M.; Brus, L. *Acc. Chem. Res.* **1999**, 32, 407–414.
- Achermann, A.; Hollingsworth, J. A.; Klimov, V. I. *Phys. Rev. B* **2003**, 68, 2453021–5.
- Nann, T.; Mulvaney, P. *Angew. Chem.* **2004**, 116, 5511; Nann, T.; Mulvaney, P. *Angew. Chem., Int. Ed.* **2004**, 43, 5393.
- Hess, B. C.; Okhrimenko, I. G.; Davis, R. C.; Stevens, B. C.; Schulzke, Q.; Wright, K. C.; Bass, C. D.; Evans, C. D.; Summers, S. L. *Phys. Rev. Lett.* **2001**, 86, 3132–5.
- Rodriguez-Viejo, J.; Mattoussi, H.; Heine, J. R.; Kuno, M. K.; Michel, J.; Bawendi, M. G.; Jensen, K. F. *J. Appl. Phys.* **2000**, 87, 8526–34.

- (23) Van Sark, W. G.; Frederix, P. L.; Van den Heuvel, D. J.; Gerritsen, H. C.; Bol, A. A.; van Lingen, J. N. J.; de Mello Donegá, C.; Meijerink, A. *J. Phys. Chem. B* **2001**, *105*, 8281–4.
- (24) Grundmann, M.; Bimberg, D. *Phys. Rev. B* **1997**, *55*, 9740–5.
- (25) Leatherdale, C. A.; Woo, W.-K.; Mikulec, F. V.; Bawendi, M. G. *J. Phys. Chem. B* **2002**, *106*, 7619–22.
- (26) Klimov, V. I.; McBranch, D. W. *Phys. Rev. B* **1997**, *55*, 13173–9.
- (27) Burda, C.; Link, S.; Mohamed, M. B.; El-Sayed, M. A. *J. Chem. Phys.* **2002**, *116*, 3828–33.
- (28) Banin, U.; Bruchez, M.; Alivisatos, A. P.; Ha, T.; Weiss, S.; Chemla, D. S. *J. Chem. Phys.* **1999**, *110*, 1195–1201.
- (29) Caruge, J.-M.; Chan, Y.; Sundar, V.; Eisler, H. J.; Bawendi, M. G. *Phys. Rev. B* **2004**, *70*, 0853161–7.
- (30) Kuno, M.; Fromm, D. P.; Johnson, S. T.; Gallagher, A.; Nesbitt, D. J. *Phys. Rev. B* **2003**, *67*, 1253041–15.
- (31) Brokmann, X.; Hermier, J.-P.; Messin, G.; Desbiolles, P.; Bouchaud, J.-P.; Dahan, M. *Phys. Rev. Lett.* **2003**, *90*, 1206011–4.
- (32) Chung, I.; Bawendi, M. G. *Phys. Rev. B* **2004**, *70*, 1653041–5.